HHS Public Access

Author manuscript

Oncogene. Author manuscript; available in PMC 2017 July 23.

Published in final edited form as:

Oncogene. 2017 June 22; 36(25): 3541–3552. doi:10.1038/onc.2016.497.

RARRES2 functions as a tumor suppressor by promoting β-catenin phosphorylation/degradation and inhibiting p38 phosphorylation in adrenocortical carcinoma

Yi Liu-Chittenden[1], **Meenu Jain**[1], **Kelli Gaskins**[1], **Sophie Wang**[1], **Maria J. Merino**[2], **Shweta Kotian**[1], **Sudheer Kumar Gara**[1], **Sean Davis**[3], **Lisa Zhang**[1], and **Electron Kebebew**[1]

[1]Endocrine Oncology Branch, National Cancer Institute, National Institutes of Health, Bethesda, Maryland [2]Laboratory of Pathology, National Cancer Institute, National Institutes of Health, Bethesda, Maryland [3]Cancer Genetics Branch, Center for Cancer Research, National Cancer Institute, Bethesda, Maryland

Abstract

Tumor suppressor genes and the immune system are critical players in inhibiting cancer initiation and/or progression. However, little is known about whether a tumor suppressor gene can function through both immune-dependent and -independent mechanisms. Retinoic acid receptor responder 2 (*RARRES2*) is transcriptionally downregulated in multiple cancer types. Previous studies suggested that it can serve as an immune-dependent tumor suppressor by acting as a chemoattractant to recruit anti-cancer immune cells expressing its receptor, the chemerin chemokine receptor 1 (CMKLR1), to sites of tumor. In this study, we investigated the role of RARRES2 in adrenocortical carcinoma (ACC), a rare lethal malignancy in which aberrant Wnt/β-catenin signaling is frequently detected. We show that *RARRES2* expression is downregulated in ACC as compared to normal and benign adrenocortical tissues, which is a result of CpG hypermethylation. Despite minimal CMKLR1 expression and lack of phenotypic tumor-suppressive effect with exogenous RARRES2 treatment, RARRES2 overexpression in ACC cell lines not only reduced cell proliferation, cell invasion and tumorigenicity *in vitro*, but also inhibited tumor growth *in vivo* in two immunodeficient mouse xenograft models. Mechanistically, RARRES2 overexpression in ACC cells inhibited Wnt/β-catenin pathway activity by promoting β-catenin phosphorylation and degradation, it also inhibited the phosphorylation of p38 mitogen-activated protein kinase. Thus our study identifies RARRES2 as a novel tumor suppressor for ACC, which can function through an immune-independent mechanism.

Address all correspondence and requests for reprints to: Electron Kebebew, MD, Endocrine Oncology Branch, National Cancer Institute, National Institutes of Health, 10 Center Drive, Room 4-5952, Bethesda, MD 20892-1201. Phone: 301-496-5049, Fax: 301-402-1788, kebebewe@mail.nih.gov.

Disclosure statement: The authors have nothing to disclose.

CONFLICT OF INTEREST

The authors declare no conflict of interest.

Keywords

RARRES2; tumor suppressor; beta-catenin; p38 MAPK; adrenocortical carcinoma

INTRODUCTION

Cancer initiation and progression are the consequence of cumulative genetic and epigenetic alterations. Such alterations, especially in proto-oncogenes, will disrupt tissue homeostasis and lead to tumor formation.[1] The human body has comprehensive strategies to combat cancer initiation and/or progression. On one hand, numerous tumor-suppressor genes are in place to counteract the tumorigenicity resulting from oncogenic activation.[1] On the other hand, the immune system also plays a role in tumor destruction and preventing cancer progression.[2] However, little is known about whether a tumor suppressor gene can function through both immune-dependent and -independent antitumor mechanisms.

Adrenocortical carcinoma (ACC) is a rare and aggressive malignancy with an estimated incidence of 0.7–2.0 cases per million people per year and a five-year overall survival rate ranging from 32% to 47%.[3–5] Various genetic alterations have been identified in ACC which might lead to the pathogenesis of ACC, among which, one of the most frequently observed event is the constitutive activation of the Wnt/β-catenin signaling pathway.[6] Although lots of studies have been done to identify oncogenic mechanisms of ACC, little is known about whether there are any tumor suppressor genes that could counteract the development of ACC.

Retinoic acid receptor responder protein 2 (RARRES2), also known as chemerin, was first identified as a secreted ligand for the orphan G protein-coupled receptor chemokine-like receptor 1 (CMKLR1).[7, 8] RARRES2 can function as a chemoattractant by recruiting immune cells expressing CMKLR1 to lymphoid organs and sites of tissue injury, thus playing an important role in immune response.[7, 9–11] Recent data also support the idea that RARRES2 can function as an adipokine, which regulates adipocyte development and metabolism by signaling through CMKLR1.[12, 13] Growing evidence suggest that RARRES2 might also play a role in cancer development. The *RARRES2* gene has been found to be transcriptionally downregulated in adrenocortical carcinoma (ACC), skin squamous cell carcinoma, melanoma, human hepatocellular carcinoma (HCC), and in lung, breast, colon and metastatic prostate cancers as compared to normal and/or benign tumors in each organ.[14–19] Recent studies suggest that RARRES2's function in cancer is associated with its chemoattractant ability. For example, in human HCC, reduced RARRES2 protein expression in tumor tissues was associated with lower infiltration of dendritic cells and natural killer (NK) cells;[17] while in melanoma, RARRES2 was shown to play an indirect role in tumor suppression by recruiting CMKLR1-expressing NK cells to tumor sites in order to carry out an antitumor effect.[18] In this study, we provide evidence that RARRES2 has a direct tumor-suppressive effect that does not require immune cell recruitment to be executed. We showed that RARRES2 was downregulated in ACCs, which was due to gene hypermethylation. RARRES2 overexpression *in vitro* led to reduced cell proliferation, cell invasion, and tumorigenicity. Using mouse xenografts of ACC cell lines with stable RARRES2

overexpression in two immunodeficient mouse models, we showed that RARRES2 expression alone was sufficient for suppressing tumor growth. Mechanistically, RARRES2 overexpression promoted the phosphorylation and degradation of β-catenin, which is associated with reduced Wnt/β-catenin pathway activity; it also inhibited the phosphorylation of p38 mitogen-activated protein kinase (MAPK). Thus, we present the first evidence that RARRES2 can function as a tumor suppressor in ACC through a novel immune-independent mechanism.

RESULTS

CpG Hypermethylation Suppresses *RARRES2* Expression in ACC

In our previous genome-wide methylation profiling study in adrenocortical tissues,[19] we found that *RARRES2* was significantly hypermethylated in ACCs as compared to benign adrenocortical tumors and normal adrenocortical samples. Significant hypermethylation was detected at five CpG sites (cg11327659, cg 13722127, cg19310340, cg21521758 and cg274550017), three of which were located in the body of the gene, while the other two were located in the 5′ UTR region (Figure 1a). The methylation at the CpG site, cg11327659, was validated by pyrosequencing in 8 ACC tissues and 42 benign tissues (Figure 1b). To further validate that methylation did occur at these five sites, and to assess their impact on *RARRES2* gene expression, we treated three ACC cell lines (NCI-H295R [H295R], SW13, and BD140A) and HEK293 cells with decitabine (DAC), a DNA methyltransferase inhibitor. In all four cell lines, DAC treatment led to a significant reduction in methylation at all five CpG sites (Figure 1c), with dose-dependent increases in *RARRES2* gene expression levels (Figure 1d). These findings suggest that, in ACC, *RARRES2* expression is suppressed by CpG hypermethylation, a common mechanism of gene silencing in cancer.[20]

RARRES2 Expression is Significantly Downregulated in ACCs

To determine if *RARRES2* is differentially expressed in adrenocortical tissues, TaqMan real-time quantitative PCR (qPCR) was performed in 21 normal adrenocortical tissues, 68 benign adrenocortical tumors, and 26 ACCs. *RARRES2* expression was significantly downregulated in ACCs as compared to benign and normal tissues. It was also significantly downregulated in benign tumors as compared to normal tissues (Figure 2a). Further, we analyzed *RARRES2* gene expression in two publically available adrenocortical databases (NCBI-GEO dataset accession no. GSE10927[21] and European Bioinformatics Institute [EMBL-EBI] accession no. E-TABM-311[22]) and found lower *RARRES2* expression in ACCs (Figure 2b and 2c). To examine RARRES2 protein expression in adrenocortical tissues, immunohistochemical (IHC) staining for RARRES2 was performed in adrenocortical tissue sections from 10 normal, 56 benign and 19 ACC samples and total signal intensity for each slide was scored. Compared to normal adrenocortical tissues, RARRES2 protein expression was significantly lower in benign tumors, and even lower in ACC samples, which is consistent with the mRNA expression profiles we observed (Figure 2d and 2e). In 9 normal, 48 benign and 15 ACC tissue samples with paired gene expression data by qPCR and protein expression data by IHC, a correlation analysis was performed. RARRES2 mRNA expression

was significantly correlated with protein expression in these adrenocortical tissue samples (r=0.3194, P = 0.0062) (Figure 2f).

RARRES2 Overexpression Inhibits Cell Proliferation, Cell Invasion and Tumorigenesis *in Vitro*

Since ACCs had significantly reduced *RARRES2* expression, and the endogenous gene expression levels of *RARRES2* and *CMKLR1* were barely detectable in all the cell lines we tested, including three ACC cell lines (Figure 3a), we decided to overexpress RARRES2 to assess its physiological function. After transient transfection, RARRES2 expression was strongest and most sustained in HEK293 cells, moderate in H295R cells, and weakest in SW13 cells (Figure 3b). The RARRES2 protein level was not detected in BD140A cells after transfection (data not shown). Transient RARRES2 overexpression led to significantly reduced cell proliferation in HEK293 cells, and reduced cell invasion in H295R cells and HEK293 cells, but had no significant effect on cell migration (Figure 3c–3e).

In order to test the long-term effect of RARRES2 expression in ACC cells, we generated stable polyclonal ACC cell lines expressing either an empty vector or RARRES2. One empty vector cell line and two independently-derived RARRES2-expressing cell lines, namely, Line-1 and Line-2, were tested. Compared to the vector cell line, RARRES2-overexpressing Line-1, but not Line-2, showed significant growth inhibition (Figure 4a). Interestingly, Line-1 had a consistently higher expression of RARRES2 than Line-2 (Figure 4b); thus, the growth suppression observed was RARRES2-dose-dependent. Importantly, both RARRES2-overexpressing cell lines showed dramatically inhibited tumorigenicity as exemplified by reduced colony formation in clonogenic assays (Figure 4c) and anchorage-independent growth in soft agar colony formation assays (Figure 4d), and the extent of inhibition was also correlated with the expression level of RARRES2. Consistent with the transient transfection result, stable RARRES2 overexpression significantly reduced cell invasion, but did not reduce the migration of H295R cells (Figure 4e and 4f).

Extracellular RARRES2 Does Not Exhibit Any Phenotypic Effect

Since RARRES2 is known as a secreted protein, and most of its known function is thought to be through the binding of its receptor, CMKLR1, we wonder if residual CMKLR1 expression in these cells could still mediate the growth-suppressive effect we observed *in vitro*. To test this hypothesis, we examined whether exogenous addition of recombinant RARRES2 protein would have any functional impact *in vitro*. Recombinant human chemerin was added to the culture media of H295R, SW13, and HEK293 cells at various physiological concentrations. However, we did not observe any significant changes in cell proliferation or cell invasion/migration (Supplementary Figure S1).

RARRES2 Overexpression Promotes Beta-Catenin Phosphorylation and Degradation, and Inhibits p38 MAPK Phosphorylation

To identify the mechanism behind the tumor-suppressive effect of RARRES2, we performed a phosphokinase array in the stable cell lines. RARRES2 overexpression led to significantly reduced total β-catenin levels and phospho-p38 MAPK levels (Figure 5a). These results were further confirmed by Western blot analysis (Figure 5b).

The reduction in β-catenin protein levels was not due to a decrease in gene expression, because TaqMan real-time qPCR of the stable cell lines revealed no significant changes in β-catenin transcription levels when RARRES2 was overexpressed (Figure 5c). Thus, these results suggested that β-catenin downregulation may be due to post-translational mechanism(s). To test if the reduction in total β-catenin is caused by phosphorylation and subsequent proteasome-mediated degradation, the cells were treated with MG132, a known proteasome inhibitor.[23] Compared to the control dimethyl sulfoxide (DMSO) treated cells, which exhibited a minimally detectable phospho-β-catenin signal, MG132 treatment successfully blocked proteasome-mediated degradation, thus allowing the phosphorylated β-catenin to be detected (Figure 5d). Compared to the vector control, RARRES2 overexpression promoted β-catenin phosphorylation at Ser33/Ser37/Thr41, leading to increased proteasome-mediated degradation, as a result, a reduced total β-catenin level. To observe this effect *in situ*, immunofluorescent staining was performed in H295R cells transiently transfected with either an empty vector or a RARRES2-overexpression construct, so that cells with different levels of RARRES2 expression could be compared. RARRES2 expression was mostly cytoplasmic with some membrane localization. Overexpression of RARRES2 led to uniform reduction of total β-catenin levels in the cells (Figure 5e).

To determine if the reduced total β-catenin level resulting from RARRES2 overexpression could affect the activity of the Wnt/β-catenin pathway, a T-cell factor/lymphoid enhancer factor (TCF/LEF) luciferase reporter assay was performed in the stable cell lines. Consistent with total β-catenin levels in the cell lines, the TCF/LEF reporter activity was also reduced in the RARRES2-overexpressing cell lines as compared to the Vector cell line (Figure 5f). We further performed cell line mutational analysis in all ACC cell lines in order to examine if there are any mutations in Wnt/β-catenin pathway related genes that could affect the activity of this pathway. Only H295R cells harbored a heterozygous S45P mutation in *CTNNB1* (Supplementary Table 1).

To determine if the phosphorylation change in p38 MAPK is physiologically relevant in ACC, IHC staining for phospho-p38 was performed. Nuclear localized phospho-p38 signal was detected in 21 of 30 ACC samples tested (70%) (Figure 5g). The relative expression level of phospho-p38 was further studied in a subset of adrenocortical tissue samples containing 8 normal, 8 benign and 8 local recurrent ACC tissues. Interestingly, phospho-p38 to p38 ratio was significantly higher in ACC as compared to normal and benign tissues (Figure 5h).

Since RARRES2 overexpression led to reduced cellular invasion, we also tested if RARRES2 expression would affect extracellular matrix (ECM) protein levels, which are major protein mediators of cellular invasion. The expression of five common cell adhesion molecules (fibronectin, collagen I, collagen IV, laminin I, fibrinogen) were not detected in H295R cells regardless of RARRES2 expression in an ECM cell adhesion array (data not shown). However, we did find that the level of N-cadherin decreased significantly when RARRES2 was overexpressed (Figure 5b).

RARRES2 Overexpression Suppresses Tumor Growth in Mouse Xenograft Models

To examine the function of RARRES2 *in vivo*, we performed xenograft studies using two different immunodeficient mouse models: athymic nude and NOD *Scid* gamma (NSG) mice. Stable H295R cells that were expressing either an empty vector or RARRES2 (Line-1) were injected subcutaneously into both flanks of the mice. In both models, RARRES2 overexpression significantly suppressed tumor growth (Supplementary Figure S2a and Figure 6a) and resulted in lower tumor weight (Supplementary Figure S2b and S2c, Figure 6b and 6c). *RARRES2* expression in the tumors was confirmed by TaqMan real-time qPCR (Supplementary Figure S2d and Figure 6d), and the xenograft tumors from RARRES2-overexpressing cell line had comparable RARRES2 protein levels as in normal human adrenocortical tissues (Figure 6e). Since the athymic nude mice are T-cell deficient, but are not B-cell and NK-cell deficient, they still have a residual immune response. To test if the tumor suppression of the RARRES2-overexpressing tumor was the result of CMKLR1-expressing immune cell recruitment, we examined the mouse *CMKLR1* expression level in the tumors that were isolated from the control and RARRES2 expression group. No significant difference in mouse *CMKLR1* expression was observed between the groups (Supplementary Figure S2e). The NSG mouse models are more immunodeficient because they have no mature T cells, B Cells and NK cells and are macrophage and dendritic cell-defective;[24, 25] nonetheless, we tested mouse *CMKLR1* expression in tumors isolated from these mice and found no difference between the groups (Figure 6f). Consistent with the observation *in vitro*, NSG mice tumors with RARRES2 overexpression showed reduced total β-catenin and reduced phospho-p38 MAPK levels (Figure 6g).

DISCUSSION

In this study, we provide evidence that RARRES2 is downregulated in ACC as a result of CpG hypermethylation. We also show that RARRES2 can function as a tumor suppressor independently of its chemoattractive ability. RARRES2 overexpression not only led to reduced cell proliferation, cell invasion, and reduced tumorigenicity *in vitro*, but also dramatically inhibited tumor growth *in vivo* in two immunodeficient mouse models.

We studied the mechanisms by which RARRES2 may have the phenotypic effects we observed *in vitro* and *in vivo*. We found that RARRES2 overexpression lead to reduced total β-catenin levels in H295R cells in a RARRES2-dose-dependent manner. This is consistent with a recent study reported by Salomon A. *et al.*, since RARRES2 overexpression recapitulates many of the phenotypes exhibited by loss of β-catenin in the H295R cells, such as reduced cell proliferation and reduced anchorage-independent growth.[29] We then examined the cause of β-catenin reduction and the potential impact on the Wnt/β-catenin pathway. In the canonical Wnt/β-catenin pathway, when Wnt is absent, cytoplasmic β-catenin is sequestered within a complex that contains the scaffolding protein axin, the tumor suppressor adenomatous polyposis coli, glycogen synthesis kinase 3 (GSK3) and casein kinase 1 (CK1α).[30] CK1α phosphorylates β-catenin at Ser45, which primes it for the subsequent phosphorylation at Thr41, Ser37 and Ser33 by GSK3.[31] The E3 ubiquitin ligase β-Trcp recognizes the phosphorylated β-catenin and targets it for proteasome degradation. When Wnt is present, the axin-mediated β-catenin phosphorylation and degradation is

disrupted, allowing β-catenin to enter and accumulate in the nucleus, where it serves as a transcriptional coactivator for the TCF/LEF family of transcription factors and turns on Wnt-responsive target genes.[30] H295R cells harbor a heterozygous β-catenin mutation on the CK1α phosphorylation site (Ser45Pro), resulting in constitutive TCF-dependent transcription.[32] By mutation analysis of the cell lines used in the current study, we confirmed the existence of such mutation in H295R cells. We also showed that RARRES2 overexpression could enhance β-catenin phosphorylation at Ser33/Ser37/Thr41, thus promoting the degradation of the β-catenin protein. Using a TCF/LEF luciferase reporter assay, we confirmed that loss of total β-catenin levels reflected the reduction in Wnt/β-catenin pathway activity. These results are particularly significant since the activation of the Wnt/β-catenin signaling pathway is observed in 54% of adrenocortical tumors, and β-catenin activation is associated with higher tumor grades, decreased overall survival, and decreased disease-free survival in patients with ACC.[32, 33] Wnt/β-catenin pathway activation has been observed in both benign ACAs and ACCs;[32] however, it is unknown why the same pathway alteration(s) results in different benign and malignant tumors. We showed that RARRES2 is downregulated in ACCs as compared to ACAs and normal adrenocortical tissues. Through pyrosequencing, we also confirmed that epigenetic CpG hypermethylation is a cause of RARRES2 downregulation in ACCs. Since RARRES2 can promote β-catenin phosphorylation and degradation, thus affecting Wnt/β-catenin pathway activity, reduced RARRES2 expression in ACCs may be a contributing factor for cancer initiation in ACAs.

The p38 MAPK signaling pathway has been shown to play dual roles in human cancers. Depending on the context, it can be pro-apoptotic, acting as a tumor suppressor by promoting cell death and inhibiting malignant transformation; it can also be pro-tumorigenic, acting as an oncogene by promoting cancer cell survival, proliferation, invasion/migration and regulating cancer metabolism.[34, 35] Activation of p38 signaling is positively correlated with bad prognosis in cancers.[35] In our study, we found that RARRES2 overexpression led to reduced phosphorylation of p38 both *in vitro* and *in vivo*. IHC staining in ACCs revealed that phospho-p38 signal is present in most tumor samples. We also found that phospho-p38/total p38 levels were significantly higher in ACC as compared to normal and benign samples. To our knowledge, our data present the first evidence that the p38 MAPK pathway might be physiologically relevant to the development of ACCs. The increase in phospho-p38/total p38 levels observed in ACC might be associated with decreased RARRES2 expression.

Currently, RARRES2 is recognized as a secreted protein that can bind to three known receptors, including CMKLR1, chemokine(C-C motif) receptor-like 2 and G protein-coupled receptor 1.[7, 26, 27] CMKLR1 is the only functional receptor that mediates RARRES2's known function in inflammation, obesity, and immune-dependent tumor suppression.[8, 18, 28] However, in our study, we showed that RARRES2 overexpression alone can lead to reduced tumorgenicity both *in vitro* and *in vivo* in two immunodeficient mouse models. These experiments provided evidence that RARRES2 can function as an immune-independent tumor suppressor. It is unclear whether this immune-independent tumor-suppressive role of RARRES2 functions through CMKLR1 since endogenous *CMKLR1* gene expression levels were barely detectable in all the cell lines we tested, and no significant phenotypic effect was observed when the cells was treated with commercially

available recombinant RARRES2 protein. There are several possible reasons that the commercially available recombinant RARRES2 fails to elicit the same phenotype as the overexpressed protein. First, the half-life of the recombinant protein might be too short to induce a phenotype. Second, it is *E.coli*-derived, which might have different posttranslational modification than those produced by human cells, which might affect its activity. Third. RARRES2 is translated as a 163 amino acid proprotein,[7] while the commercially available recombinant protein is a cleaved form that contains only amino acids 21–157. Although this cleaved protein is active in inducing chemotaxis of immune cells through CMKLR1, it is not known whether the cleaved form will be enough to induce the tumor-suppressive effect found in our study. It is possible that RARRES2 does not need to function through a receptor to carry out its tumor suppressive function. In fact, from IHC in human tissue samples and immunofluorescence staining in RARRES2-overexpessing cells, we observed that RARRES2 is mainly located in the cytoplasm, which suggests that it might have other function as a cytosolic protein.

Whether RARRES2 exhibits a direct or indirect tumor-suppressive role might be tissue specific. It is also possible that the immune-dependent and -independent tumor-suppressive roles of RARRES2 are not mutually exclusive. However, the downregulation of *RARRES2* gene expression was observed in multiple human malignancies such as skin squamous cell carcinoma, HCC, and in lung, breast and colon cancers.[16–18] Interestingly, abnormal Wnt/β-catenin activity has also been observed in human squamous cell carcinoma, HCC, breast cancers and lung cancers.[36] In breast and lung cancers, Wnt signaling is hyperactive despite rare pathway mutations.[36] In lung cancers and high grade colon cancers, aberrant activation of p38 signaling has been reported.[37, 38] These findings prompt us to speculate that the direct tumor-suppressive effect of RARRES2 might not be limited to ACCs. In fact, transient RARRES2 overexpression in HEK293 cells showed reduction in cell proliferation and invasion, which supports this speculation. It would be interesting to test the role of RARRES2 in the other cancers.

In summary, we present, for the first time, evidence that RARRES2 can function as a tumor suppressor in ACC in an immune-independent manner. RARRES2 is a unique tumor suppressor that possesses both immune-dependent and -independent tumor-suppressive abilities.

MATERIALS AND METHODS

Patient Samples

Human adrenocortical tissue samples were collected according to an institutional review board–approved clinical protocol after written informed consent was obtained (NCT01005654 and NCT01348698).

Cell Lines, Transfection, and Recombinant Protein Treatment

Human ACC cell lines H295R and SW13 were purchased from ATCC (Rockville, MD), cultured in DMEM supplemented with 1% insulin transferrin selenium and 2.5% NuSerum I (Corning, Bedford, MA), and authenticated by short-tandem repeat profiling. The BD140A

ACC cell line was kindly provided by Drs. Kimberly Bussey and Michael Demeure (TGen, Pheonix, AZ), and was cultured in RPMI-1640 medium supplemented with 10% FBS, 1% penicillin-streptomycin, and 1% L-glutamate (Life Technologies, Grand Island, NY). Human embryonic kidney cell line HEK293 was cultured in DMEM supplemented with 10% FBS (Sigma-Aldrich) and 1% penicillin-streptomycin. All cell lines were maintained in a standard humidified incubator with 5% CO_2 at 37°C. All cell lines had been recently authenticated by STR profiling and tested for mycoplasma contamination.

For transient transfection, the RARRES2 plasmid (SC118329, pCMV-XL5-RARRES2) and empty vector (pCMV-XL5) were obtained from Origene (Rockville, MD). Mirus TransIT-2020 (Mirus Bio LLC, Madison, WI) was used for transfecting ACC cell lines, while X-tremeGENE HP (Roche, Indianapolis, IN) was used for transfecting HEK293. To establish the RARRES2-overexpressing stable cell lines, RARRES2 cDNA from pCMV-XL5-RARRES2 was cloned into the pcDNA4/Myc-His A vector (Life Technologies) to generate pcDNA4-RARRES2 so that only the un-tagged protein was expressed. pcDNA4-RARRES2 was linearized with BglII (New England Biolabs, Ipswich, MA) and was transfected into H295R cells in six-well plates. Three days after transfection, the selection marker Zeocin (Life Technologies) was added to the cell culture medium at 1 μg/ml. The medium with Zeocin was changed twice a week until the drug-resistant clones grew. Cells from one six-well were pooled as one polyclonal line and were maintained in selection medium. A stable cell line established by transfecting H295R cell line with a BglII-linearized pcDNA4/Myc-His A vector was used as the vector control.

Recombinant human chemerin protein was obtained from R&D systems (Minneapolis, MN, 2324-CM-025), and reconstituted according to the manufacturer's protocol.

Decitabine Treatment and Pyrosequencing

Decitabine (5-Aza-2′-deoxycytidine, Sigma-Aldrich, A3656) was diluted in DMSO to the desired concentration. Cells were seeded in triplicate in six-well plates, treated with decitabine or the DMSO vehicle for 72 hours (HEK293, SW13, BD140A) or 144 hours (H295R) after cell attachment. The genomic DNA from cells was isolated with the DNeasy Blood & Tissue kit (Qiagen, Valencia, CA). Bisulfite conversion of genomic DNA, primer design, PCR and pyrosequencing were performed by the Genomics Lab at the Frederick National Laboratory for Cancer Research (Frederick, MD).

RNA Isolation, cDNA Synthesis, and TaqMan Real-Time Quantitative PCR

Total RNA was isolated using the TRIzol reagent (Life Technologies) according to the manufacturer's protocol. It was then reverse-transcribed using the High Capacity cDNA Reverse Transcription Kit (Applied Biosystems, Foster City, CA). TaqMan real-time qPCR was performed on the Applied Biosystems 7900HT fast real-time PCR systems. Unless mentioned otherwise, the expression of the gene of interest was presented as the percentage of the gene expression of housekeeping gene *GAPDH* ($=2\text{^}-[Ct_{\text{Target gene}}-Ct_{\text{GAPDH}}]*100$). The reaction was prepared by mixing cDNA, TaqMan 2x universal PCR master mix, and TaqMan gene expression assays (Applied Biosystems). The gene expression assays used

were: RARRES2 (Hs0016120_g1), CMKLR1 (Hs01081979_s1), mouse CMKLR1 (Mm01700212_m1), CTNNB1 (Hs00355049_m1), and GAPDH (Hs99999905_m1).

Immunohistochemistry (IHC)

Tissue-section slides were de-paraffinized in xylene and rehydrated in ethanol, followed by antigen retrieval with 10% citrate buffer (pH 6.0) in a pressure cooker for 10 minutes at 120 °C. Slides were incubated with the primary antibody at 4°C overnight. For RARRES2 staining, tissues were fixed with 10% formalin and embedded in paraffin. Anti-chemerin antibody (Abcam, Cambridge, MA, ab72965) was used at 12.5 μg/ml. Immunostaining was performed using the Dako Envison+ System-HRP (DAB) for mouse primary antibodies (Dako, Carpinteria, CA). IHC slides were scored using the formula Total staining intensity = Σ (intensity scores × percent positivity), where intensity score 0 = no staining, 1 = weak staining, 2 = moderate staining, 3 = strong staining. Interpreter of the IHC was blind to the diagnosis and gene expression levels accessed by real-time qPCR. For phospho-p38 staining, primary antibody used was phospho-p38 (Thr180/Tyr182) antibody (1: 800, Cell Signaling, Danvers, MA, #4511). Immunostaining was performed by detection with SignalStain Boost IHC detection reagents (HRP, Cell signaling, rabbit #8114), followed by staining with Vector DAB peroxidase (HRP) substrate kit (Vector laboratories, Burlingame, CA, SK-4100). Hematoxylin (Sigma-Aldrich, St. Louis, MO) was used for counterstaining.

Cell Proliferation, Invasion and Migration

Cell proliferation experiments were performed using CyQUANT cell proliferation assays (Life Technologies) according to the manufacturer's protocol. For transiently transfected cells, the cells were first transfected in six-well plate, trypsinized 24 hours later, counted, and then seeded at least in quadruplicate on ninety-six-well black plates to monitor growth. Absorbance at 485 nm/538 nm was determined using a ninety-six-well fluorescence microplate reader SpectraMax M5 (Molecular Devices, Sunnyvale, CA). H295R cells were seeded at 8,000 cells/well, HEK293 cells at 3,000 cells/well, and SW13 at 6,000 cells/well. Four independent experiments were performed for each cell line.

Cell invasion and migration assays were performed using the BioCoat Matrigel Invasion chamber and control chamber (Corning, Corning, NY) according to the manufacturer's protocol. Cells were seeded in duplicate at 1 × 10^5 cells/insert. Transiently transfected cells were first transfected in six-well plate, then trypsinized and seeded at 24 hours after transfection. Stably transfected cells were seeded directly. The plates were then incubated at 37°C to allow for cell invasion/migration. ACC cells were incubated for 44 hours, while HEK293 cells were incubated for 22 hours. Inserts were then fixed and stained with Diff-Quik (Dade Behring, Newark, NJ). Images of the stained inserts were taken under a light microscope and quantified using Image J software (National Institutes of Health, Bethesda, MD). For invasion, the cell number in the entire insert was counted. For migration, the cell number in four random fields of one insert was counted and summed. For each experiment, invasion/migration was measured as the ratio of total invaded/migrated RARRES2-overexpressing cells to cells expressing the empty vector. The final figure represents collective results from four independent experiments for the transiently transfected cells and

three independent experiments for the stably transfected cells. Paired t-test was used to compare difference between each group.

Clonogenic Assay and Crystal Violet Staining

A solution of 0.1% Gelatin (Sigma-Aldrich) in PBS was used to coat six-well plates and was discarded after half an hour. Stable H295R cells were seeded at 5 000 cells/well and cultured for 3 weeks until the colonies reached optimal size. After discarding the cell culture medium, the cells were fixed with a 4% paraformaldehyde solution (Affymetrix, Santa Clara, CA) at room temperature for 15 minutes, and then stained with 0.05% Crystal violet (Fisher Scientific, Fair Lawn, NJ) in distilled H_2O for 30 minutes. The plates were rinsed with water and air dried. Pictures were taken using the ProteinSimple FluorChem E Imaging system. Cells were

Soft Agar Colony Formation Assay

Cell culture medium containing 0.7% agarose (Life Technologies) was added into six-well plates at 1.5 ml/well as the bottom layer. After the bottom layer solidified, another 1.5 ml of culture medium containing 0.4% agarose and 2 ×10^4 cells was added on top. The plates were then kept in the cell culture incubator for 3–4 weeks. Colonies were visualized and pictures were taken under an Olympus SZX9 microscope. Cells were seeded in triplicate in each experiment, and the experiments were repeated three times.

Phosphokinase Array

A phosphokinase array was performed using the Proteome Profiler Human Phosphokinase Array (R&D Systems), according to the manufacturer's protocol. Stable cell lines were cultured in 10 cm tissue culture dishes until ~80% confluency, and then the lysate was collected for the assay.

Western Blotting

A lysis buffer with 1% of SDS,10 mM of Tris HCl (pH 7.4), and supplemented with 1× Halt protease inhibitor cocktail and 1× Halt phosphatase inhibitor cocktail (Thermo Fisher Scientific) was used. The primary antibodies used were: RARRES2 antibody (1:1 000, Abcam, ab72965); GAPDH antibody (1: 5 000, Santa Cruz Biotechnology, sc-47724), β-catenin antibody (1:1 000, Cell Signaling, #8480), phospho-β-catenin (Ser33/37/Thr41) antibody (1: 1 000, Cell signaling, #9561), phospho-p38 (Thr180/Tyr182) antibody (1:1 000, Cell Signaling, #4511), p38 antibody (1:1 000, Cell Signaling, #8690). Secondary antibodies used were goat anti-mouse IgG-horseradish peroxidase (HRP) and goat anti-rabbit IgG-HRP (1:5 000, Santa Cruz Biotechnology). Except for Western blots including multiple tissue samples, each Western blot experiments were repeated three times with independent sample sets.

Immunofluorescence Staining

H295R cells were seeded in 6-well plate at 1x10^6 cells/well the day before transfection. On the second day, cells were transiently transfected with 1 μg of empty vector (pCMV-XL5) or RARRES2-expressing construct (pCMV-XL5-RARRES2). Two days after transfection, the

cells were trypsinized and transferred to a fresh 6-well plate with cell culture medium and a glass coverslip in the well. One day later, the cells were fixed with 4% paraformaldehyde solution (Affymetrix, Cleveland, OH) for 15 minutes and proceeded with immunofluorescent staining. Primary antibodies used were: RARRES2 antibody (5 μg/ml, Abcam, ab72965), β-catenin antibody (1: 100, Cell Signaling, #8480). Secondary antibodies used were: Alexa Fluor 594 goat anti-mouse IgG (H+L) and Alexa Fluor 488 goat anti-rabbit IgG (H+L) (1:500, Life Technologies). Coverslips were mounted on slides with Vectashield mounting medium for fluorescence with DAPI (Vector Laboratories, H-1200). Images were taken using Zeiss LSM 780 confocal microscope with a 63x objective. Three independent experiments were performed and representative images were shown.

TCF/LEF Reporter Assay

TCF/LEF reporter assay was carried out using Cignal TCF/LEF Reporter (luc) Kit (Qiagen, CCS-018L), followed by luciferase measurement using Dual-Glo Luciferase Assay System (Promega, Madison, WI, E2920). Plate readings were measured by SpectraMax M5. Stable H295R cell lines (Vector, Line-1 and Line-2) were seeded at 5000 cells/well in 96-well in quadruplicates one day before transfection. On the second day, the cells were transfected with 0.1 μg of either the TCF/LEF transcription factor reporter, which contained a 40:1 mixture of inducible TCF/LEF responsive firefly luciferase reporter and constitutively expressing Renilla reporter, or the negative control, which contains a 40:1 mixture of non-inducible firefly luciferase reporter and constitutively expressing Renilla reporter. Two days after transfection, Dual-Glo luciferase assay reagent was added to each well per the manufacturer's protocol. TCF/LEF luciferase activity in each cell line was then measured as the ratio of firefly luciferase activity of the TCF/LEF reporter to the negative control. The final figure represents collective results from three independent experiments. Paired t-test was used to compare difference between each group.

Mice Xenograft

Female athymic nude mice (2–3 months old) were obtained from the Frederick National Laboratory for Cancer Research animal facilities (Frederick, MD). NOD.Cg-*Prkdc*^{scid}*Il2rg*^{tm1Wjl}/SzJ (NOD *scid* gamma, NSG) breeder mice were purchased from The Jackson Laboratory, and were maintained and bred according to the guidelines of the National Institutes of Health Animal Research Advisory Committee (NIH-ARAC). NSG mice (five females and two males) were xenografted when they were 3–4 months old. Mice were randomly assigned to two groups, each group receiving a subcutaneous injection on both sides of the flank with 3 ×10^6 H295R cells stably expressing either RARRES2 or the control vector in a 100-μl suspension (cell culture medium: Matrigel =1:1). A blinded measurement of the tumor size was taken each week. Tumor volumes were calculated using the equation $x^2y/2$, where x is the smallest and y is the largest diameters. Mice were sacrificed when the tumor size reached 2 cm in greatest diameter. For NSG mice, there were seven mice (fourteen xenografts) in each group, but one xenograft in the RAR group never developed into measurable tumor, thus was excluded from the following analysis. The animal experiments were approved by the NIH-ARAC.

Statistical Analysis

All statistical analyses were performed using GraphPad Prism 6.0 (La Jolla, CA). Unless otherwise specified, data are presented as mean ± SD. Unless otherwise specified, unpaired t-tests were used to compare difference between different groups. A two-tailed P value of < 0.05 was considered statistically significant.

Supplementary Material

Refer to Web version on PubMed Central for supplementary material.

Acknowledgments

This work was supported by the intramural research program of the Center for Cancer Research, National Cancer Institute, National Institutes of Health (1ZIABC01127506).

References

1. Sherr CJ. Principles of tumor suppression. Cell. 2004; 116:235–246. [PubMed: 14744434]
2. Finn OJ. Immuno-oncology: understanding the function and dysfunction of the immune system in cancer. Annals of oncology : official journal of the European Society for Medical Oncology / ESMO. 2012; 23(Suppl 8):viii6–9.
3. Bilimoria KY, Shen WT, Elaraj D, Bentrem DJ, Winchester DJ, Kebebew E, et al. Adrenocortical carcinoma in the United States: treatment utilization and prognostic factors. Cancer. 2008; 113:3130–3136. [PubMed: 18973179]
4. Kerkhofs TM, Verhoeven RH, Van der Zwan JM, Dieleman J, Kerstens MN, Links TP, et al. Adrenocortical carcinoma: a population-based study on incidence and survival in the Netherlands since 1993. European journal of cancer (Oxford, England : 1990). 2013; 49:2579–2586.
5. Fassnacht M, Allolio B. Clinical management of adrenocortical carcinoma. Best practice & research Clinical endocrinology & metabolism. 2009; 23:273–289. [PubMed: 19500769]
6. Fassnacht M, Kroiss M, Allolio B. Update in adrenocortical carcinoma. The Journal of clinical endocrinology and metabolism. 2013; 98:4551–4564. [PubMed: 24081734]
7. Wittamer V, Franssen JD, Vulcano M, Mirjolet JF, Le Poul E, Migeotte I, et al. Specific recruitment of antigen-presenting cells by chemerin, a novel processed ligand from human inflammatory fluids. The Journal of experimental medicine. 2003; 198:977–985. [PubMed: 14530373]
8. Ernst MC, Sinal CJ. Chemerin: at the crossroads of inflammation and obesity. Trends in endocrinology and metabolism: TEM. 2010; 21:660–667. [PubMed: 20817486]
9. Wittamer V, Bondue B, Guillabert A, Vassart G, Parmentier M, Communi D. Neutrophil-mediated maturation of chemerin: a link between innate and adaptive immunity. J Immunol. 2005; 175:487–493. [PubMed: 15972683]
10. Zabel BA, Silverio AM, Butcher EC. Chemokine-like receptor 1 expression and chemerin-directed chemotaxis distinguish plasmacytoid from myeloid dendritic cells in human blood. J Immunol. 2005; 174:244–251. [PubMed: 15611246]
11. Vermi W, Riboldi E, Wittamer V, Gentili F, Luini W, Marrelli S, et al. Role of ChemR23 in directing the migration of myeloid and plasmacytoid dendritic cells to lymphoid organs and inflamed skin. The Journal of experimental medicine. 2005; 201:509–515. [PubMed: 15728234]
12. Goralski KB, McCarthy TC, Hanniman EA, Zabel BA, Butcher EC, Parlee SD, et al. Chemerin, a novel adipokine that regulates adipogenesis and adipocyte metabolism. The Journal of biological chemistry. 2007; 282:28175–28188. [PubMed: 17635925]
13. Bozaoglu K, Bolton K, McMillan J, Zimmet P, Jowett J, Collier G, et al. Chemerin is a novel adipokine associated with obesity and metabolic syndrome. Endocrinology. 2007; 148:4687–4694. [PubMed: 17640997]

14. Velazquez-Fernandez D, Laurell C, Geli J, Hoog A, Odeberg J, Kjellman M, et al. Expression profiling of adrenocortical neoplasms suggests a molecular signature of malignancy. Surgery. 2005; 138:1087–1094. [PubMed: 16360395]
15. Fernandez-Ranvier GG, Weng J, Yeh RF, Khanafshar E, Suh I, Barker C, et al. Identification of biomarkers of adrenocortical carcinoma using genomewide gene expression profiling. Archives of surgery (Chicago, Ill : 1960). 2008; 143:841–846. discussion 846.
16. Zheng Y, Luo S, Wang G, Peng Z, Zeng W, Tan S, et al. Downregulation of tazarotene induced gene-2 (TIG2) in skin squamous cell carcinoma. European journal of dermatology : EJD. 2008; 18:638–641. [PubMed: 18955196]
17. Lin W, Chen YL, Jiang L, Chen JK. Reduced expression of chemerin is associated with a poor prognosis and a lowed infiltration of both dendritic cells and natural killer cells in human hepatocellular carcinoma. Clinical laboratory. 2011; 57:879–885. [PubMed: 22239017]
18. Pachynski RK, Zabel BA, Kohrt HE, Tejeda NM, Monnier J, Swanson CD, et al. The chemoattractant chemerin suppresses melanoma by recruiting natural killer cell antitumor defenses. The Journal of experimental medicine. 2012; 209:1427–1435. [PubMed: 22753924]
19. Rechache NS, Wang Y, Stevenson HS, Killian JK, Edelman DC, Merino M, et al. DNA methylation profiling identifies global methylation differences and markers of adrenocortical tumors. The Journal of clinical endocrinology and metabolism. 2012; 97:E1004–1013. [PubMed: 22472567]
20. Baylin SB. DNA methylation and gene silencing in cancer. Nat Clin Pract Oncol. 2005; 2(Suppl 1):S4–11. [PubMed: 16341240]
21. Giordano TJ, Kuick R, Else T, Gauger PG, Vinco M, Bauersfeld J, et al. Molecular classification and prognostication of adrenocortical tumors by transcriptome profiling. Clinical cancer research : an official journal of the American Association for Cancer Research. 2009; 15:668–676. [PubMed: 19147773]
22. de Reynies A, Assie G, Rickman DS, Tissier F, Groussin L, Rene-Corail F, et al. Gene expression profiling reveals a new classification of adrenocortical tumors and identifies molecular predictors of malignancy and survival. Journal of clinical oncology : official journal of the American Society of Clinical Oncology. 2009; 27:1108–1115. [PubMed: 19139432]
23. Palombella VJ, Rando OJ, Goldberg AL, Maniatis T. The ubiquitin-proteasome pathway is required for processing the NF-kappa B1 precursor protein and the activation of NF-kappa B. Cell. 1994; 78:773–785. [PubMed: 8087845]
24. Ishikawa F, Yasukawa M, Lyons B, Yoshida S, Miyamoto T, Yoshimoto G, et al. Development of functional human blood and immune systems in NOD/SCID/IL2 receptor {gamma} chain(null) mice. Blood. 2005; 106:1565–1573. [PubMed: 15920010]
25. Shultz LD, Lyons BL, Burzenski LM, Gott B, Chen X, Chaleff S, et al. Human lymphoid and myeloid cell development in NOD/LtSz-scid IL2R gamma null mice engrafted with mobilized human hemopoietic stem cells. J Immunol. 2005; 174:6477–6489. [PubMed: 15879151]
26. Barnea G, Strapps W, Herrada G, Berman Y, Ong J, Kloss B, et al. The genetic design of signaling cascades to record receptor activation. Proceedings of the National Academy of Sciences of the United States of America. 2008; 105:64–69. [PubMed: 18165312]
27. Zabel BA, Nakae S, Zuniga L, Kim JY, Ohyama T, Alt C, et al. Mast cell-expressed orphan receptor CCRL2 binds chemerin and is required for optimal induction of IgE-mediated passive cutaneous anaphylaxis. The Journal of experimental medicine. 2008; 205:2207–2220. [PubMed: 18794339]
28. Bondue B, Wittamer V, Parmentier M. Chemerin and its receptors in leukocyte trafficking, inflammation and metabolism. Cytokine & growth factor reviews. 2011; 22:331–338. [PubMed: 22119008]
29. Salomon A, Keramidas M, Maisin C, Thomas M. Loss of beta-catenin in adrenocortical cancer cells causes growth inhibition and reversal of epithelial-to-mesenchymal transition. Oncotarget. 2015; 6:11421–11433. [PubMed: 25823656]
30. MacDonald BT, Tamai K, He X. Wnt/beta-catenin signaling: components, mechanisms, and diseases. Dev Cell. 2009; 17:9–26. [PubMed: 19619488]

31. Kimelman D, Xu W. beta-catenin destruction complex: insights and questions from a structural perspective. Oncogene. 2006; 25:7482–7491. [PubMed: 17143292]
32. Tissier F, Cavard C, Groussin L, Perlemoine K, Fumey G, Hagnere AM, et al. Mutations of beta-catenin in adrenocortical tumors: activation of the Wnt signaling pathway is a frequent event in both benign and malignant adrenocortical tumors. Cancer research. 2005; 65:7622–7627. [PubMed: 16140927]
33. Gaujoux S, Grabar S, Fassnacht M, Ragazzon B, Launay P, Libe R, et al. beta-catenin activation is associated with specific clinical and pathologic characteristics and a poor outcome in adrenocortical carcinoma. Clinical cancer research : an official journal of the American Association for Cancer Research. 2011; 17:328–336. [PubMed: 21088256]
34. Igea A, Nebreda AR. The Stress Kinase p38alpha as a Target for Cancer Therapy. Cancer research. 2015; 75:3997–4002. [PubMed: 26377941]
35. Grossi V, Peserico A, Tezil T, Simone C. p38alpha MAPK pathway: a key factor in colorectal cancer therapy and chemoresistance. World journal of gastroenterology : WJG. 2014; 20:9744–9758. [PubMed: 25110412]
36. Polakis P. Wnt signaling in cancer. Cold Spring Harb Perspect Biol. 2012:4.
37. Wagner EF, Nebreda AR. Signal integration by JNK and p38 MAPK pathways in cancer development. Nature reviews Cancer. 2009; 9:537–549. [PubMed: 19629069]
38. Chiacchiera F, Grossi V, Cappellari M, Peserico A, Simonatto M, Germani A, et al. Blocking p38/ERK crosstalk affects colorectal cancer growth by inducing apoptosis in vitro and in preclinical mouse models. Cancer letters. 2012; 324:98–108. [PubMed: 22579651]

a

CpG site	Location relative to coding region	ACC vs. Benign			ACC vs. Normal		
		M-value difference	Beta-value difference	Adjusted p-value	M-value difference	Beta-value difference	Adjusted p-value
cg11327659	Body	2.08	0.32	1.84E-08	1.62	0.25	2.06E-05
cg13722127	5'UTR	1.40	0.22	1.74E-05	1.36	0.21	1.02E-04
cg19310340	Body	1.59	0.24	2.41E-07	1.50	0.23	4.21E-06
cg21521758	Body	1.73	0.27	5.51E-08	1.56	0.24	2.97E-06
cg27455017	5'UTR	1.97	0.30	5.88E-06	1.74	0.27	1.84E-04

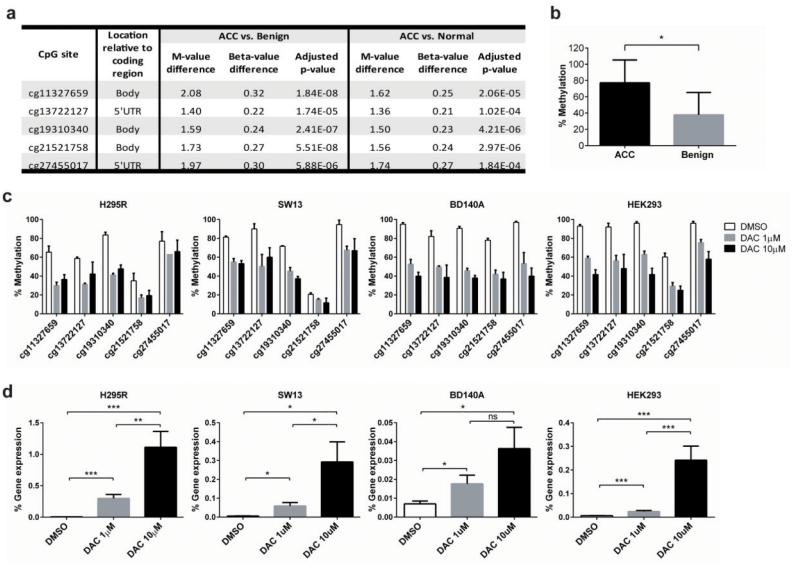

Figure 1.

Epigenetic CpG hypermethylation suppresses *RARRES2* expression in adrenocortical tumors. (**a**) Five CpG sites in *RARRES2* were significantly methylated in ACCs as compared to benign and normal adrenocortical tissue samples. ACC, n = 8; benign, n = 47; normal, n = 19. M-value, the log2 ratio of the intensities of methylated probe versus unmethylated probe. Beta-value, the ratio of the methylated probe intensity and the overall (methylated and unmethylated) probe intensity. (**b**) Pyrosequencing validation of the methylation status for the CpG site cg11327659. ACC, n = 8; benign, n = 42. *, $P < 0.0005$. (**c**) Pyrosequencing results revealed that decitabine treatment significantly reduced *RARRES2* methylation in the 5 targeted CpG sites in cultured H295R, SW13, BD140A and HEK293 cells. (**d**) Decitabine treatment increases *RARRES2* gene expression in cultured H295R, SW13, BD140A and HEK293 cells as detected by TaqMan qPCR. *, $P < 0.05$; **, $P < 0.01$; ***, $P < 0.005$. (**c**) and (**d**), Due to the longer cell doubling time, H295R were treated for 144 hours, while the other cell lines were treated for 72 hours.

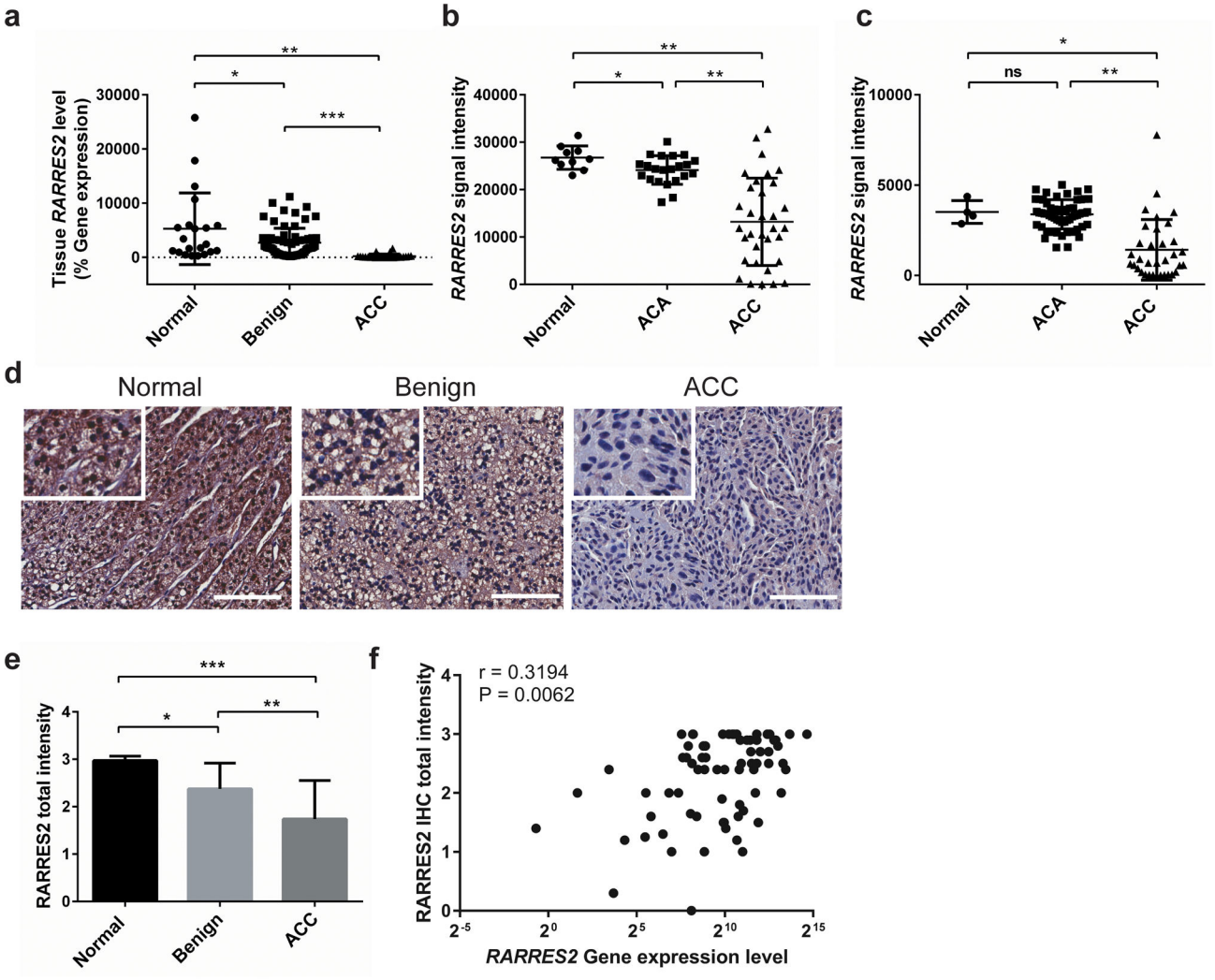

Figure 2.

RARRES2 expression is significantly downregulated in adrenocortical carcinomas. (**a**) TaqMan real-time qPCR result confirms *RARRES2* downregulation in ACCs in our cohort of adrenocortical tissue samples. Normal, n = 21; Benign, n = 68; ACC, n = 26. *, $P < 0.05$; **, $P < 0.0005$; ***, $P < 0.0001$. (**b**) *RARRES2* expression in publicly available microarray data from the GEO database (accession no. GSE10927). ACA, adrenocortical adenoma. Normal, n = 10; ACA, n = 22; ACC, n = 33. *, $P < 0.05$; **, $P < 0.0001$. (**c**) *RARRES2* expression in publicly available microarray data from EMBL-EBI (accession no. E-TABM-311). Normal, n = 4; ACA, n = 58; ACC, n = 34. *, $P < 0.05$; **, $P < 0.0001$; ns, not significant. (**a**) – (**c**), Individual tissue samples were represented by dots. Long horizontal lines represent the means; short horizontal lines represent the SD. (**d**) Representative IHC staining images for RARRES2 in adrenocortical tissues. Scale bars, 100 μm. Inset, zoom in images. (**e**) Quantification of RARRES2 staining intensity in adrenocortical tissues. Normal, n = 10; Benign, n = 56; ACC, n = 19. Intensity scores: 0, no staining; 1, weak staining; 2, moderate staining, 3, strong staining. Total staining intensity = Σ (intensity scores × percent positivity). *, $P < 0.005$; **, $P < 0.0005$; ***, $P < 0.0001$. (f) Correlation between tissue

RARRES2 mRNA expression level, measured by Taqman qPCR as % gene expression relative to GAPDH, and RARRES2 protein level, as scored from IHC. r, correlation coefficient. Paired RNA and tissue slides from 9 normal, 48 benign and 15 ACC tissues were analyzed.

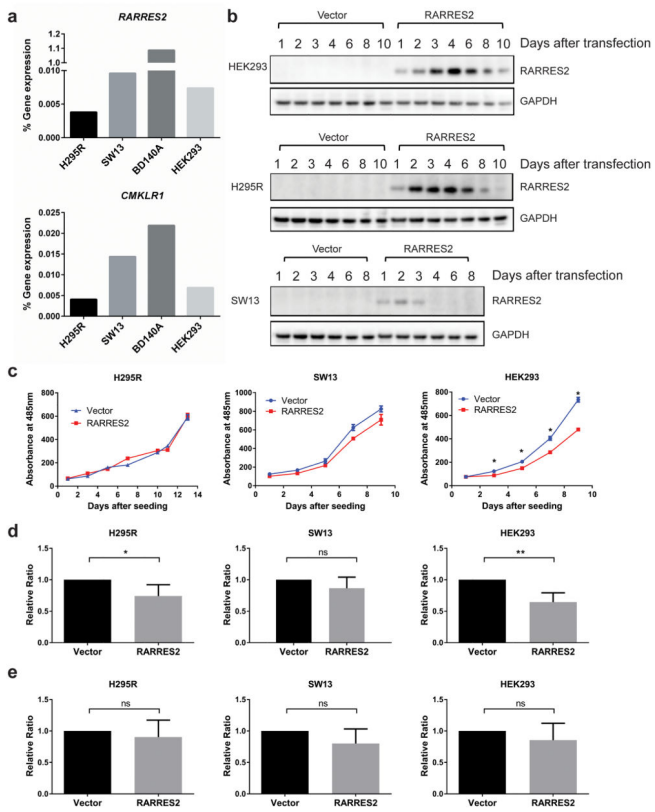

Figure 3.

Transient RARRES2 overexpression inhibits cell proliferation in HEK293 cells and leads to reduced cellular invasion in H295R and HEK293 cells. (**a**) Baseline RARRES2 and CMKLR1 gene expression levels were barely detectable in the cell lines tested using TaqMan qPCR. (**b**) The time course for RARRES2 expression after transient transfection in HEK293, H295R and SW13 cell lines. (**c**) *in vitro* cell proliferation curve for cell lines transiently transfected with a vector control or RARRES2. Transient overexpression of RARRES2 inhibited cell proliferation in HEK293 cells, but not in H295R or SW13 cells. Data were presented as mean ± SEM. *, $P < 0.0001$. (**d**) Transient RARRES2 expression inhibits cellular invasion in H295R cells and HEK293 cells but not in SW13 cells. *, $P < 0.05$; **, $P < 0.01$; ns, not significant. (**e**) Transient RARRES2 expression does not affect cell migration. No significant difference was observed between cells transfected with vector or RARRES2.

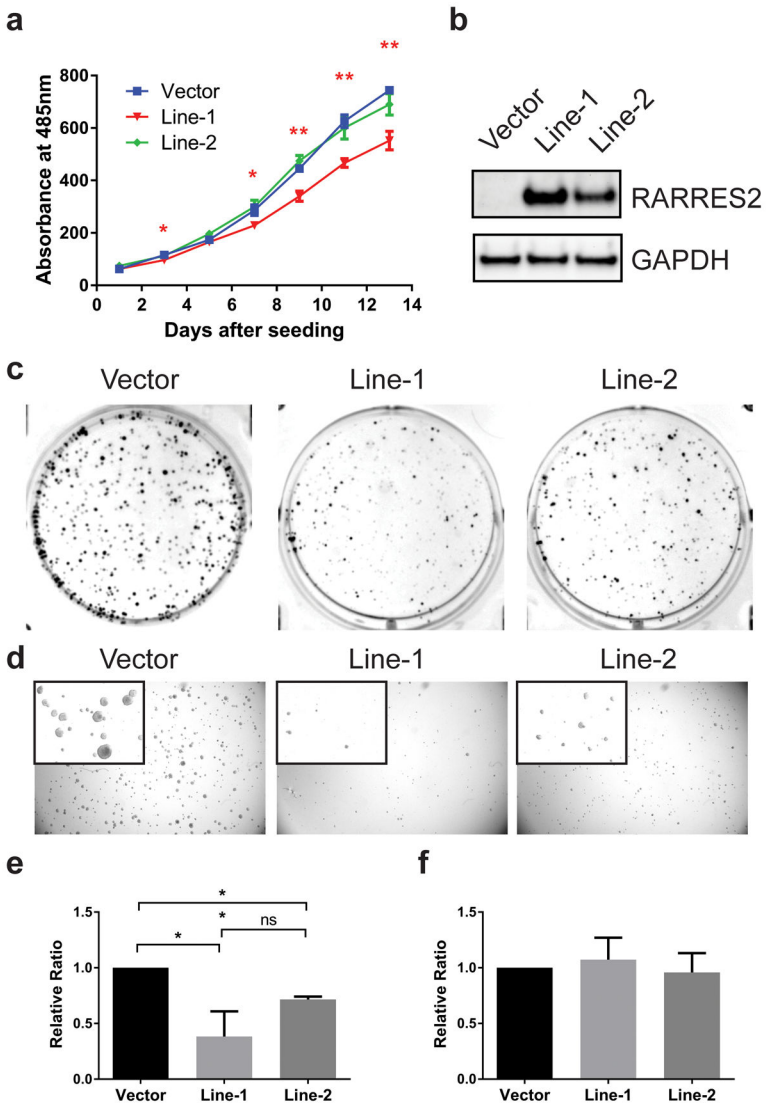

Figure 4.

Stable RARRES2 overexpression in H295R shows a dose-dependent tumor-suppressive effect. (**a**) *in vitro* cell proliferation curve for cell lines stably transfected with a vector control or RARRES2. Three polyclonal cell lines expressing either an empty vector or RARRES2 (Line-1 and Line-2) were tested. Data were presented as mean ± SEM. *, $P < 0.05$; **, $P < 0.005$. (**b**) RARRES2 expression in stable H295R cell lines as detected by Western blot analysis. Line-1 had consistently higher RARRES2 expression than Line-2. (**c**) Stable RARRES2 overexpression inhibits the clonogenic ability of H295R in colony formation assays. Representative images of colony formation in 6-well plates are shown. (**d**) Stable RARRES2 overexpression inhibits anchorage-independent growth of H295R in soft agar colony assays. Representative bright-field images are shown. Inset, zoomed-in images of the colonies. (**e**) Stable RARRES2 overexpression reduces cell invasion. *, $P < 0.05$; **, $P < 0.005$; ns, not significant. (**f**) Stable RARRES2 overexpression does not affect cell migration.

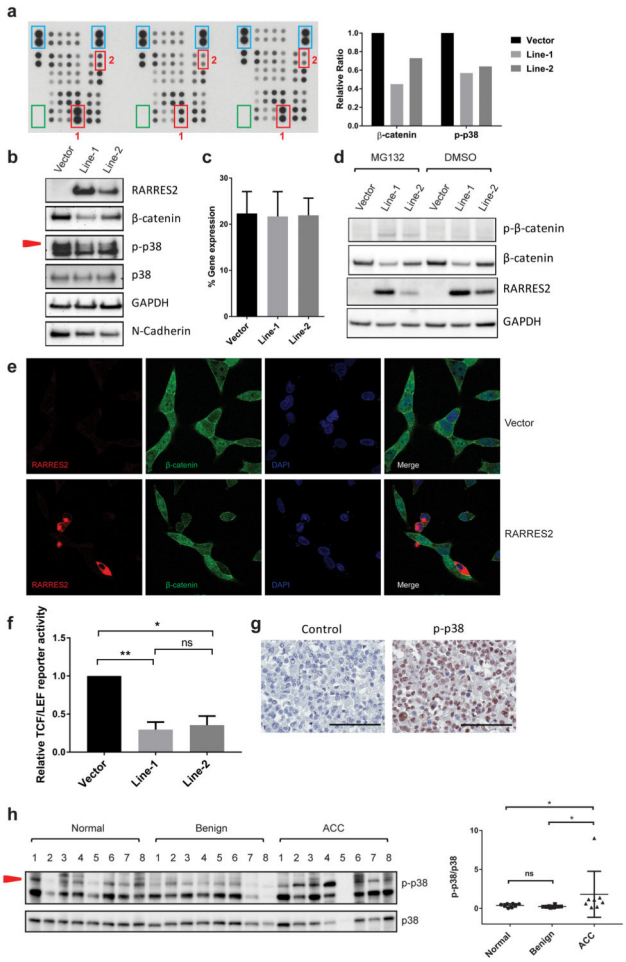

Figure 5.

RARRES2 overexpression promotes β-catenin phosphorylation and degradation, and reduces p38 MAPK phosphorylation. (**a**) Reduced total β-catenin and phospho-p38 MAPK (p-p38) were identified by human phosphokinase array kit. Left: film image of the array membranes. For each membrane, antibodies for each protein tested are printed in vertically aligned duplicates. Positive reference spots are shown in blue boxes. Negative controls are shown in green boxes. RARRES2-dose-dependent reduction was seen in total β-catenin (red box 1) and p-p38 (red box 2). Right: relative intensity of target (phospho-) proteins in each cell line. (**b**) Western blot validation of the phosphokinase array result. (**c**)The β-catenin transcript level is not affected by RARRES2 overexpression based on TaqMan real-time qPCR. Results are obtained from cDNAs isolated from seven independent experiments. (**d**) RARRES2 overexpression promotes β-catenin phosphorylation and degradation in a dose-dependent manner. Stable H295R cell lines were treated with 20 μM MG132 for 6 hours, followed by Western blot analysis. Note that the MG132 treatment resulted in the detection of phospho-β-catenin at Ser33/Ser37/Thr41. (**e**) Representative images of immunofluorescence staining of transiently transfected H295R cell lines. Top panel, cells transfected with empty vector. Bottom panel, cells transfected with RARRES2-expressing construct. Overexpression of RARRES2 (red) *in situ* led to reduced total β-catenin (green)

levels. Cell nuclei were stained blue with DAPI. (**f**) Relative TCF/LEF luciferase reporter activity among stable H295R cell lines. TCF/LEF luciferase activity of RARRES2-overexpresing Line-1 and Line-2 were normalized to the Vector line. *, $P < 0.05$; **, $P < 0.01$; ns, not significant. (**g**) Representative image of IHC staining for p-p38 in ACC. Left panel, negative control with no p-p38 primary antibody added. Right panel, representative image of p-p38 staining in ACC. Scale bar, 100 μm. (**h**) Western blot analysis in human adrenocortical tissues. Left panel, protein lysates from eight each of normal, benign and local recurrent ACC tissues with adequate frozen tissue samples were analyzed. Red arrow head points to the protein band corresponding to p-p38. Right panel, densitometry analysis of relative intensity of p-p38/total p38 levels in each group. *, $P < 0.05$; ns, not significant.

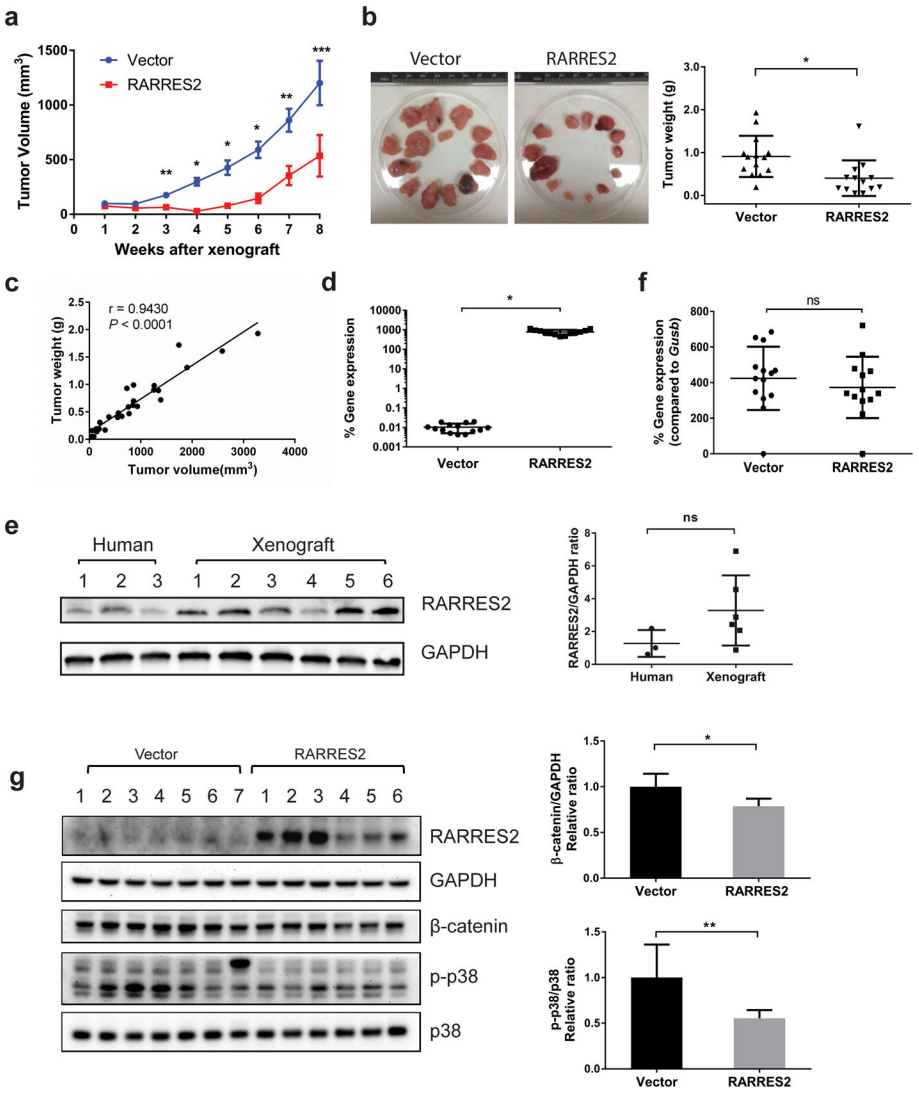

Figure 6.

RARRES2 overexpression inhibits tumor growth in an NSG mice xenograft model. (**a**) The tumor growth curve in NSG mice. RARRES2 overexpression resulted in a significant growth inhibition as compared to the vector group starting from 3 weeks after xenograft. Each group contains seven mice / fourteen xenografts, but in the RARRES2 group, one xenograft never developed a measurable tumor, thus was excluded. Data were presented as mean ± SEM. *, $P < 0.0001$, **, $P < 0.005$, ***, $P < 0.05$. (**b**) The tumors isolated from each group at the time of sacrifice (8 weeks after xenograft). Left panel, pictures of all the tumors isolated from each group. Right panel, the tumor weight in each group. (**c**) The correlation between tumor volume and tumor weight for all tumors isolated (n = 27). r, correlation coefficient. (**d**) The human *RARRES2* gene expression level in tumors isolated as measured by TaqMan qPCR. *, $P < 0.0001$. (**e**) RARRES2 protein level comparison between normal human adrenocortical tissues and NSG mice xenograft overexpressing RARRES2. Left panel, Western blotting result of protein expression in three human normal adrenocortical tissues and six RARRES2-overexpressing NSG mice tumor xenograft samples. Right panel,

densitometry analysis of the Western blot for RARRES2/GAPDH ratio. ns, not significant. (**f**) The mouse *CMKLR1* gene expression level in tumors isolated. Note that the expression level is presented as the percentage of gene expression of the mouse housekeeping gene *Gusb*. ns, not significant. (**b**), (**d**) and (**f**), Vector, n = 14; RARRES2, n = 13. (**g**) RARRES2 expression was associated with reduced p-p38 and total β-catenin levels. Left panel, Western blotting performed in seven tumors from the vector group, and six tumors from the RARRES2 group. Arrow head points to the p-p38 band. Right panel, quantification of Western blot images. *, $P < 0.01$; **, $P < 0.05$.